

An investigation of escape and scaling properties of a billiard system

Matheus Rolim Sales,¹ Daniel Borin,¹ Diogo Ricardo da Costa,¹ José Danilo Szezech Jr.,^{2,3} and Edson Denis Leonel¹

¹*Departamento de Física, Universidade Estadual Paulista (UNESP), 13506-900, Rio Claro, SP,*

Brasil

²*Programa de Pós-Graduação em Ciências, Universidade Estadual de Ponta Grossa, 84030-900, Ponta Grossa, PR,*

Brasil

³*Departamento de Matemática e Estatística, Universidade Estadual de Ponta Grossa, 84030-900, Ponta Grossa, PR,*

Brasil

(*Electronic mail: matheusrolim95@gmail.com)

(Dated: 10 June 2024)

We investigate some statistical properties of escaping particles in a billiard system whose boundary is described by two control parameters with a hole on its boundary. Initially, we analyze the survival probability for different hole positions and sizes. We notice the survival probability follows an exponential decay with a characteristic power law tail when the hole is positioned partially or entirely over large stability islands in phase space. We find the survival probability exhibits scaling invariance with respect to the hole size. In contrast, the survival probability for holes placed in predominantly chaotic regions deviates from the exponential decay. We introduce two holes simultaneously and investigate the complexity of the escape basins for different hole sizes and control parameters by means of the basin entropy and the basin boundary entropy. We find a non-trivial relation between these entropies and the system's parameters and show that the basin entropy exhibits scaling invariance for a specific control parameter interval.

Keywords: Classical billiards, escape of particles, survival probability, scaling invariance, basin entropy

The phase space of a typical two-dimensional Hamiltonian system is not completely ergodic. There is a coexistence of chaotic and regular regions that gives rise to the well-known phenomenon of stickiness. Chaotic orbits become trapped near stability islands for long, but finite, times, and this intermittence in the chaotic motion shapes the transport and statistical properties across phase space. In this paper, we analyze the escape dynamics of a billiard system whose boundary is defined by two control parameters with an exit hole along its boundary. We find the survival probability either follows an exponential or a stretched exponential decay depending on the position of the hole. By introducing two holes simultaneously, we construct the escape basins for different hole's sizes and quantify the basins complexity using the basin entropy and the basin boundary entropy. The complexity of the basins depends nontrivially on the control parameters and we find that the basin entropy exhibits scaling invariance for a specific control parameter interval.

infinite hierarchical islands-around-islands structure, where the larger islands are surrounded by smaller islands, which are in turn surrounded by even smaller islands and so on for increasingly smaller scales^{3,4}. This complex interplay between stability islands and chaotic regions gives rise to the phenomenon of stickiness⁵⁻¹². The stickiness of chaotic orbits occurs near stability islands and these orbits experience long, but finite, periods of nearly quasiperiodic motion. Before escaping to the chaotic sea, these orbits are trapped within regions bounded by cantori^{2,4,9,13}. The cantori, which are a Cantor set, formed by the remnants of the destroyed Kolmogorov-Arnold-Moser (KAM) tori, as predicted by the KAM theorem¹, have a different function in the transport of particles in phase space than the KAM tori. While the KAM tori divide the phase space into distinct regions, the cantori act as partial barriers to the transport in phase space. The orbits may be trapped in a region bounded by the cantori, and once inside a cantorus, the chaotic orbits may transition to an inner cantorus, and so on, to arbitrarily small levels in the hierarchical structure of islands-around-islands.

The stickiness affects the statistical properties of the system, such as the decay of correlations^{6-8,14,15} and transport¹⁶⁻¹⁹. For closed systems, the transport properties may be studied considering the recurrence-time statistics (RTS)²⁰⁻²⁶, while for open systems it is customary to analyze the survival probability^{11,27-37}. For both cases, strongly chaotic dynamics leads to an asymptotic exponential decay, while in systems that exhibit stickiness, a power law tail emerges. Whether the decay follows an exponential or power law corresponds to normal or anomalous transport¹⁶⁻¹⁹, respectively.

In this paper, we study the escaping properties of a billiard system with static boundary and the scaling invariance³⁸ of some observables. Essentially, when a system exhibits scaling invariance, its expected behavior remains consistent and

I. INTRODUCTION

In general, the phase space of a typical quasi-integrable Hamiltonian system is mixed, where regular and chaotic domains coexist¹. The regular regions consist of periodic and quasiperiodic orbits that lie on invariant tori, while the chaotic orbits fill densely the whole available region in phase space. For two-dimensional area-preserving maps, the invariant tori divides the phase space into distinct and unconnected domains, *i.e.*, an orbit initially inside of an island will never reach the chaotic sea and vice versa^{1,2}. The stability islands and chaotic regions organize themselves in phase space in an

robust regardless of scale. It is explored in various systems ranging from area-preserving maps, dissipative maps and billiards as well^{39–47}, and more recently it has been explored for fractional maps^{48,49}. The billiard system with static boundary is a Hamiltonian system and it is one of the simplest dynamical systems to exhibit chaotic motion. In its two-dimensional formulation, a point-like particle is confined to a planar region Ω delimited by hard walls $\partial\Omega$. The particle undergoes elastic collisions with the boundary $\partial\Omega$ such that the angle of incidence equals the angle of reflection⁵⁰. Because billiards have a relatively simple structure, whether chaotic behavior emerges is entirely determined by the geometric characteristics of $\partial\Omega$, *i.e.*, the presence of dispersing or defocusing components in the boundary $\partial\Omega$ ⁵¹. Therefore, different billiard geometries yield different dynamical behavior, namely, fully regular⁵⁰, in which all orbits lie on periodic or quasiperiodic tori, fully chaotic^{52–54}, in which almost every orbit fills densely the entire phase space, and, mixed dynamics^{21,23,55,56}, where the phase space is composed of both regular and chaotic domains, typical of quasi-integrable Hamiltonian systems. Billiard systems have also been studied in the context of quantum^{57–61} and relativistic^{62–64} mechanics.

We consider in this paper a billiard system whose boundary depends on two control parameters. This system has been introduced in the context of quantum mechanics⁶⁵ and recently some of its classical dynamical properties have been studied⁶⁶. Our focus lies in examining the escaping properties of an ensemble of particles through a hole placed on the billiard boundary. We analyze the survival probability for different hole positions and hole sizes as well. We find that when the hole overlaps, either partially or entirely, with larger stability islands, the survival probability follows an exponential decay with a characteristic power law tail. Also, in these cases, the survival probability exhibits scaling invariance with respect to the hole size. On the other hand, when the hole is placed within a predominantly chaotic region of phase space, the survival probability deviates from this exponential decay. We extend our analysis by introducing two holes simultaneously, and we construct the escape basins for different hole sizes. We find the escape basins to be more complex, in the sense of having fewer definite structures, for smaller hole sizes. We quantify this complexity by means of the basin entropy, S_b , and the basin boundary entropy, S_{bb} ^{67,68}. We find that the larger the hole size, the smaller both entropies become, doing so in a non-trivial and intricate manner. Nonetheless, we find that for a specific parameter interval, S_b has an exponential dependence on the control parameter. Additionally, we show that S_b also exhibits scaling invariance relative to this control parameter.

This paper is organized as follows. In Section II we formally introduce billiard systems and the system under study in this paper. We also demonstrate the algorithm used to calculate the successive collisions of the particle with the billiard boundary. In Section III we introduce one hole on the billiard boundary from where the particles can escape. We calculate the survival probability for several hole sizes and positions and show that the survival probability exhibits scaling invariance when the hole is placed partially or entirely over the large

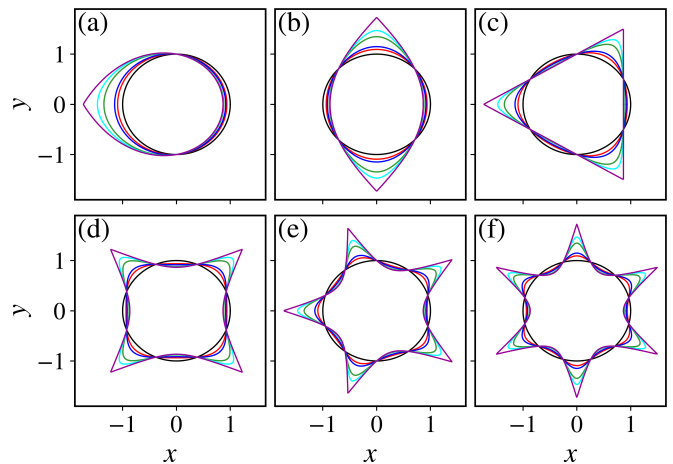


FIG. 1. The billiard boundary for (a) $\gamma = 1$, (b) $\gamma = 2$, (c) $\gamma = 3$, (d) $\gamma = 4$, (e) $\gamma = 5$, and (f) $\gamma = 6$ with different values of ξ , namely, (black) $\xi = 0.0$, (red) $\xi = 0.15$, (blue) $\xi = 0.30$, (green) $\xi = 0.75$, (cyan) $\xi = 0.90$, and (purple) $\xi = 0.99999$.

stability islands. In Section IV we consider two holes open simultaneously and construct escape basins for different hole sizes. We characterize the basins by means of the basin entropy and show that the basin entropy depends non-trivially on the hole sizes and the billiard parameters. We also show that the basin entropy exhibits scaling invariance. Section V contains our final remarks.

II. MODEL AND MAPPING

In the two-dimensional formulation of billiards, one considers a point-like particle of mass μ , or an ensemble of particles, confined in a simply connected planar region Ω delimited by hard walls $\partial\Omega$. A billiard system with static boundary is a Hamiltonian system with potential $V(\mathbf{q}) \equiv 0$ within the boundary and infinity on the boundary $\partial\Omega$, *i.e.*, its Hamiltonian function is given by

$$\mathcal{H}(\mathbf{p}, \mathbf{q}) = \frac{\mathbf{p}^2}{2\mu} + V(\mathbf{q}), \quad (1)$$

with

$$V(\mathbf{q}) = \begin{cases} 0, & \text{for } \mathbf{q} \in \Omega, \\ \infty, & \text{otherwise,} \end{cases} \quad (2)$$

where \mathbf{p} and \mathbf{q} are the generalized momentum and position, respectively. The particles undergo elastic collisions with the boundary such that only the momentum's direction is changed and the total mechanical energy of the system, $\mathcal{H}(\mathbf{p}, \mathbf{q}) \equiv E = \mathbf{p}^2/2\mu + V(\mathbf{q})$, is a constant of motion. Also, the angle of incidence equals the angle of reflection⁵⁰.

In this paper, we study a family of billiards with the boundary radius, $R(\theta)$, implicitly parameterized by^{65,66}

$$R^2 + \frac{2\sqrt{3\xi}}{9}R^3 \cos(\gamma\theta) = 1, \quad (3)$$

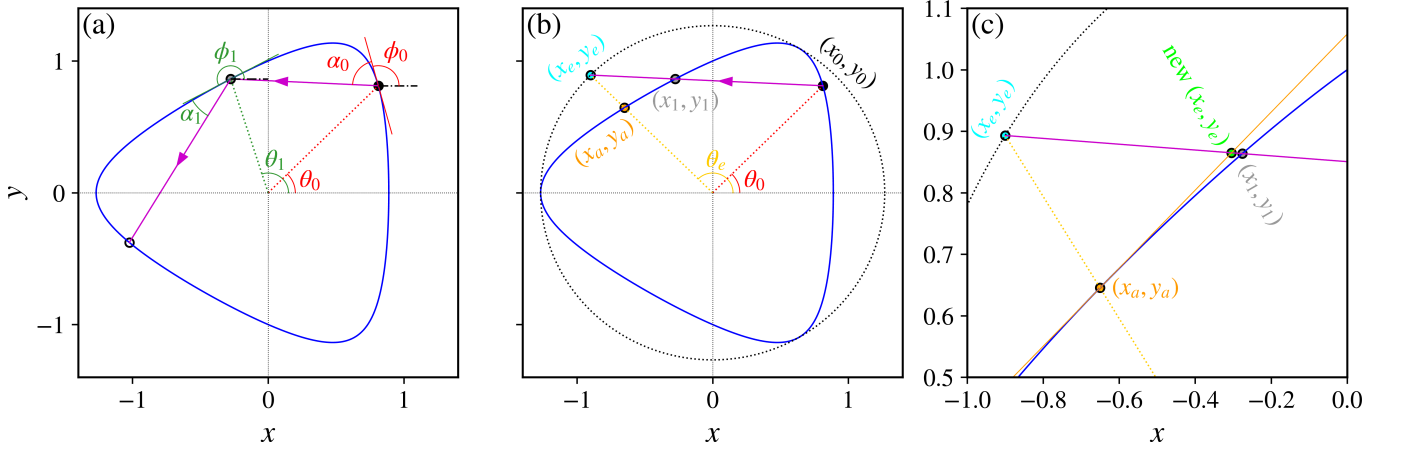


FIG. 2. (a) Illustration of the billiard boundary and the angles considered in the billiard map for $\gamma = 3$ and $\xi = 0.6$ and initial condition $(\theta_0, \alpha_0) = (\pi/4, 2\pi/5)$. Panels (b) and (c) illustrate the algorithm for finding the next collision point, as discussed in the main text.

where $\theta \in [0, 2\pi)$ is the polar angle measured counterclockwise from the horizontal axis, γ is an integer number, and $\xi \in [0, 1)$ controls the shape of the boundary. Figure 1 displays different boundary shapes for different parameter values. $\xi = 0$ yields a circular shape for all γ and $\gamma = 3$ and $\gamma = 4$ yields an equilateral triangle and a square-like shape, respectively, for $\xi \rightarrow 1$. The case $\gamma = 3$ is particularly interesting because both $\xi = 0$ and $\xi \rightarrow 1$ yield fully integrable billiard shapes.

The billiard map is a two-dimensional nonlinear mapping $\mathbb{M} : \mathbb{R}^2 \rightarrow \mathbb{R}^2$. We characterize the particle's collisions with the boundary by two angles: θ and α . The mapping relates these variables before and after the n th-collision

$$(\theta_{n+1}, \alpha_{n+1}) = \mathbb{M}(\theta_n, \alpha_n) = \mathbb{M}^n(\theta_0, \alpha_0), \quad (4)$$

where θ is the polar angle and $\alpha \in [0, \pi]$ is measured counterclockwise from the tangent line at the collision point and it is a complementary angle that measures the particle's direction of motion from the tangent line. Considering a particle initially at θ_n with initial angle α_n , the particle starts its motion from the initial point (x_n, y_n) given by, in Cartesian coordinates,

$$\begin{aligned} x(\theta_n) &\equiv x_n = R(\theta_n) \cos \theta_n, \\ y(\theta_n) &\equiv y_n = R(\theta_n) \sin \theta_n. \end{aligned} \quad (5)$$

It is convenient to define the slope ϕ of the tangent line measured counterclockwise from the horizontal axis as well. It is given by

$$\phi_n = \arctan \left[\frac{y'(\theta_n)}{x'(\theta_n)} \right] \text{ mod } 2\pi, \quad (6)$$

where the prime indicates the derivative with respect to θ . Therefore, the direction of the particle's momentum, measured counterclockwise from the horizontal axis, is

$$\mu_n = \alpha_n + \phi_n \text{ mod } 2\pi. \quad (7)$$

Since no forces are acting on the particle between two subsequent collisions the particle follows a straight line described

by the following equations:

$$\begin{aligned} x_{n+1} &= x_n + v_n \cos(\mu_n) \Delta t, \\ y_{n+1} &= y_n + v_n \sin(\mu_n) \Delta t, \end{aligned} \quad (8)$$

where Δt is the time interval between two collisions. We consider $v_n = 1$ without loss of generality and the particle's trajectory is given by

$$y(\theta_{n+1}) - y(\theta_n) = \tan(\mu_n)[x(\theta_{n+1}) - x(\theta_n)], \quad (9)$$

where θ_{n+1} is the new angular position of the particle where it hits the boundary. The direction of the particle's trajectory after the collision is given by

$$\alpha_{n+1} = \phi_{n+1} - \mu_n \text{ mod } \pi. \quad (10)$$

Therefore, the final form of the mapping \mathbb{M} is

$$\mathbb{M} : \begin{cases} F(\theta_{n+1}) = y(\theta_{n+1}) - y(\theta_n) - \\ \quad - \tan(\mu_n)[x(\theta_{n+1}) - x(\theta_n)] = 0, \\ \alpha_{n+1} = \phi_{n+1} - \mu_n \text{ mod } 2\pi. \end{cases} \quad (11)$$

Figure 2(a) shows the angles mentioned above for two subsequent collisions. Usually, the angle θ_{n+1} is obtained numerically from $F(\theta_{n+1}) = 0$ using a bisection method³¹, for example. However, in our case, we consider a more efficient algorithm to calculate θ_{n+1} ^{66,69}, which we outline shortly. This algorithm can be 25 times faster in some situations than the traditional algorithm for studying billiards⁶⁹, and it is illustrated in Figures 2(b) and 2(c). It is important to note that even though this is an efficient algorithm, it is not applicable when the boundary has convex components. In our model, the billiard shapes have no convex components for $\gamma \leq 3$ (see Figure 1), and we limit our analysis to $\gamma = 3$. For an extended and more general version of this algorithm, we refer the reader to Ref.⁶⁹.

First, we consider an external circle to the billiard boundary with radius $R_{\max} = R(\pi/\gamma)$ [dotted black line in Figures 2(b)

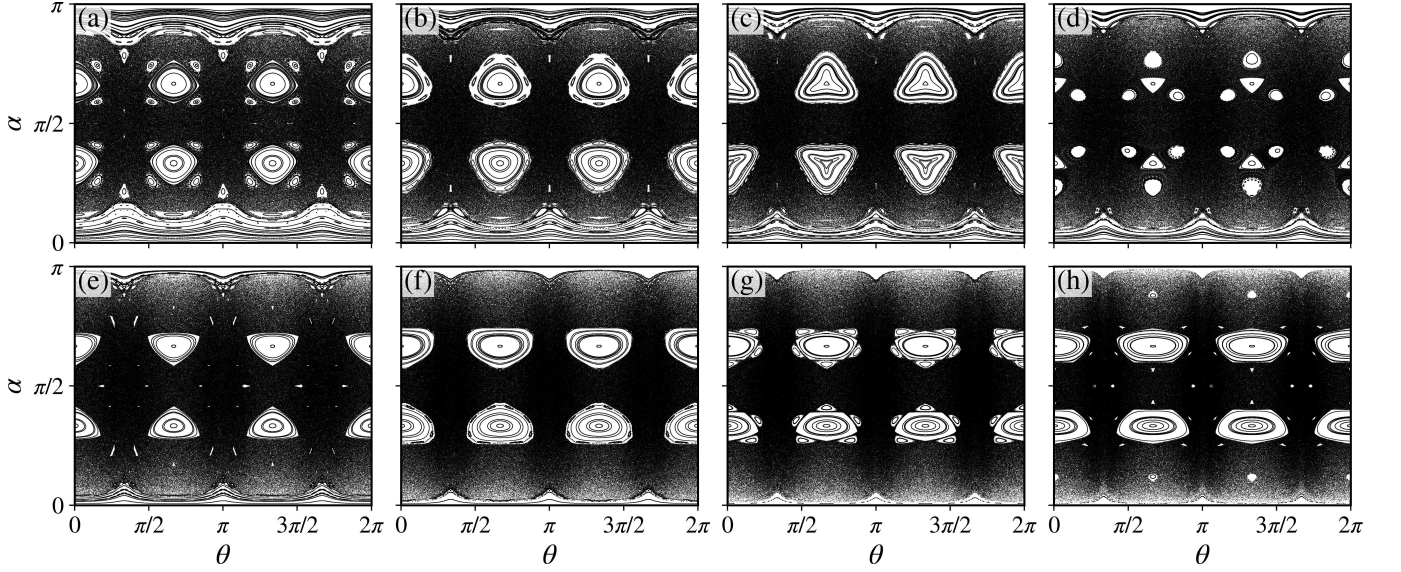


FIG. 3. The phase space for $\gamma = 3$ and (a) $\xi = 0.20$, (b) $\xi = 0.30$, (c) $\xi = 0.40$, (d) $\xi = 0.45$, (e) $\xi = 0.55$, (f) $\xi = 0.70$, (g) $\xi = 0.80$, and (h) $\xi = 0.85$.

and 2(c)]. The time it takes for the particle, initially at (x_0, y_0) [black dot in Figure 2(b)], to reach the outer circle is obtained from $x_p^2 + y_p^2 = R_{\max}^2$ [cyan dot in Figures 2(b) and 2(c)], where x_p and y_p are given by Eqs. (8). Thus, we obtain a quadratic equation for Δt

$$(\Delta t)^2 + 2[x_0 \cos \mu_0 + y_0 \sin \mu_0] \Delta t + x_0^2 + y_0^2 - R_{\max}^2 = 0, \quad (12)$$

with solution

$$\Delta t_e = \frac{-b + \sqrt{b^2 - 4c}}{2}, \quad (13)$$

where

$$\begin{aligned} b &= 2[x_0 \cos \mu_0 + y_0 \sin \mu_0], \\ c &= x_0^2 + y_0^2 - R_{\max}^2. \end{aligned} \quad (14)$$

Hence, the Cartesian coordinates (x_e, y_e) of the particle's collision point with the outer circle [cyan dot in Figures 2(b) and 2(c)] and its angular position are, respectively,

$$\begin{aligned} x_e &= x_0 + \cos(\mu_0) \Delta t_e, \\ y_e &= y_0 + \sin(\mu_0) \Delta t_e, \\ \theta_e &= \arctan\left(\frac{y_e}{x_e}\right) \bmod 2\pi. \end{aligned} \quad (15)$$

We proceed to find the position on the billiard boundary for the angle θ_e [orange dot in Figures 2(b) and 2(c)]

$$\begin{aligned} x_a &= R(\theta_e) \cos \theta_e, \\ y_a &= R(\theta_e) \sin \theta_e, \end{aligned} \quad (16)$$

and the tangent line that passes through this point (x_a, y_a) [orange line in Figure 2(c)]

$$y_t(x) = y_a + \frac{y'(\theta_e)}{x'(\theta_e)}(x - x_a). \quad (17)$$

Next, we calculate the interception of this tangent line with the particle's trajectory [lime green dot in Figure 2(c)] as $y_p = y_t(x_p)$:

$$\begin{aligned} y_0 + \sin(\mu_0) \Delta t_e^{\text{new}} &= \\ &= y_a + \frac{y'(\theta_e)}{x'(\theta_e)} [x_0 + \cos(\mu_0) \Delta t_e^{\text{new}} - x_a]. \end{aligned} \quad (18)$$

Isolating Δt_e^{new} , we obtain

$$\Delta t_e^{\text{new}} = \frac{y_a - y_0 + \frac{y'(\theta_e)}{x'(\theta_e)}(x_0 - x_a)}{\sin(\mu_0) - \frac{y'(\theta_e)}{x'(\theta_e)} \cos(\mu_0)}. \quad (19)$$

Therefore, the new interception point $(x_e^{\text{new}}, y_e^{\text{new}})$ [lime green dot in Figure 2(c)] and its angular position are given by, respectively,

$$\begin{aligned} x_e^{\text{new}} &= x_0 + \cos(\mu_0) \Delta t_e^{\text{new}}, \\ y_e^{\text{new}} &= y_0 + \sin(\mu_0) \Delta t_e^{\text{new}}, \\ \theta_e^{\text{new}} &= \arctan\left(\frac{y_e^{\text{new}}}{x_e^{\text{new}}}\right). \end{aligned} \quad (20)$$

If $|\theta_e^{\text{new}} - \theta_e| < \text{TOL}$, $|x_e^{\text{new}} - x_a| < \text{TOL}$, and $|y_e^{\text{new}} - y_a| < \text{TOL}$, with $\text{TOL} = 10^{-11}$, we consider θ_e^{new} as the angular position of the particle's collision with the billiard boundary, $\theta_1 = \theta_e^{\text{new}}$. If these conditions are not met, we repeat this procedure until the desired tolerance is achieved.

We investigate the mapping (11) along with the previously described algorithm to identify successive collisions with the boundary for $\gamma = 3$, varying the values of ξ . We examine 150 randomly selected initial conditions, iterating each one for $N = 10^4$ times [Figure 3]. The system exhibits a complex coexistence of regular and chaotic domains across all considered values of ξ , characteristic of quasi-integrable Hamiltonian systems. As ξ increases, the chaotic domain expands,

leading to the destruction of stability islands. The period-3 islands undergo multiple bifurcations and mutations. However, as ξ approaches 0.85 [Figure 3(h)], several smaller islands emerge. Beyond this threshold, the system becomes “less” chaotic, *i.e.*, the chaotic domain diminishes as $\xi \rightarrow 1$ ⁶⁶.

III. SURVIVAL PROBABILITY

In this section, we explore the properties for the escape of particles through a hole of size h , measured in the polar angle units, positioned on the billiard boundary. We consider $\gamma = 3$ and $\xi = 0.45$. Initially, we choose two distinct hole locations (Figure 4) centered at $\theta_{\text{exit}}^{(1)} = 2\pi/3$ and $\theta_{\text{exit}}^{(2)} = 5\pi/6$. We initialize an ensemble of $M = 10^6$ randomly chosen particles within the phase space region defined by $(\theta, \alpha) \in [0, \pi/3] \times [\pi/2 - 0.25, \pi/2 + 0.25]$ and iterate each particle up to $N = 10^6$ collisions⁷⁰. We keep only one hole open at a time and every time a particle collides with the exit, it escapes and we interrupt the simulation and initialize another particle. We repeat this procedure until the whole ensemble is exhausted. We compute the survival probability, $P(n)$, that corresponds to the fraction of particles that have not yet escaped through the hole until the n th collision. Mathematically, it is defined as

$$P(n) = \frac{1}{M} N_{\text{surv}}(n), \quad (21)$$

where M is the total number of particles and $N_{\text{surv}}(n)$ is the number of particles that have survived until the n th collision. It is widely known that for strongly chaotic systems, the survival probability decays exponentially^{31,33,34,36} as

$$P(n) \sim \exp(-\kappa n) \quad (22)$$

where $\kappa > 0$ is the escape rate. However, the stickiness effect affects the statistical properties of the escape of particles. For systems with mixed phase space, the decay is slower. It has been shown that for such systems, the decay is either a power law^{28,32,37} or a stretched exponential^{30,35,36}. Due to the stickiness effect, particles might be trapped near stability islands and resonance zones for a long, but finite, time leading to long escape times and causing the aforementioned deviations from the exponential decay.

In Figure 5, we present the survival probability for six different hole sizes, h , calculated considering the two hole positions shown in Figure 4. Both holes exhibit qualitatively similar behavior. For short times, the decay is exponential, while for longer times, a power-law tail emerges, which is a characteristic feature of the stickiness effect. Furthermore, κ depends on h as a power law, $\kappa(h) \sim h^z$ (Figure 6), with exponents $z_1 = 0.98680$ and $z_2 = 1.06048$ for holes #1 and #2, respectively. The knowledge of these exponents allows us to rescale the horizontal axis by the transformation $n \rightarrow nh^{z_i}$ making the survival probabilities of the corresponding holes overlap onto a single, and hence, universal plot (Figure 7).

The escape rate is larger for larger h , as expected. This leads to the following question: Is there a preferential location

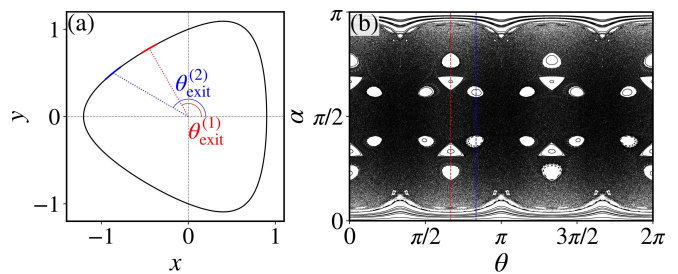


FIG. 4. (a) The billiard boundary and (b) the phase space for $\gamma = 3$ and $\xi = 0.45$. The red ($\theta_{\text{exit}}^{(1)} = 2\pi/3$) and blue ($\theta_{\text{exit}}^{(2)} = 5\pi/6$) lines in (a) on the boundary represent the holes with size $h = 0.20$. The dashed lines in (b) correspond to the positions in phase space where the holes are centered.

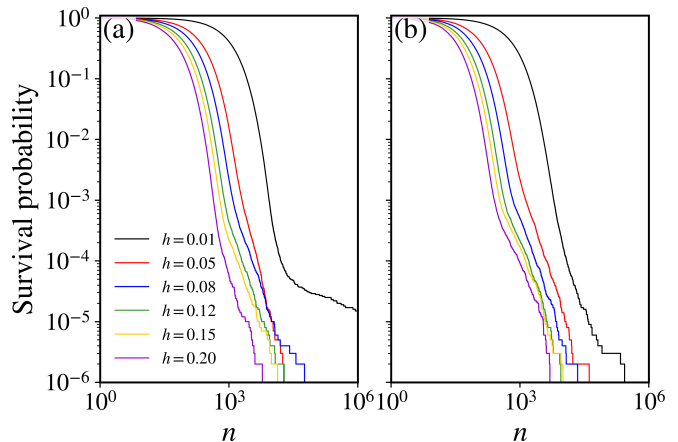


FIG. 5. The survival probability through holes (a) #1 ($\theta_{\text{exit}}^{(1)} = 2\pi/3$) and (b) #2 ($\theta_{\text{exit}}^{(2)} = 5\pi/6$) individually, for $\gamma = 3$, $\xi = 0.45$ and different values of h . We considered an ensemble of $M = 10^6$ initial conditions randomly distributed in $(\theta, \alpha) \in [0, \pi/3] \times [\pi/2 - 0.25, \pi/2 + 0.25]$.

to place the hole to enhance the escape of particles⁷¹? Insights have already been provided in Refs.^{72,73} for a different billiard system, indicating that the escape is faster when the hole is placed in regions without stability islands. Here, we observe different behaviors in the survival probability decay depending on whether the hole overlaps with one of the larger stability islands. We consider $\gamma = 3$, $\xi = 0.45$ and $h = 0.20$ and change the hole position in the interval $\theta_{\text{exit}} \in [\pi/3, \pi]$. Some holes are placed over regions with stability islands, while others are placed over regions dominated by the chaotic sea. We calculate the survival probability [Figure 8(a)] for each one of these hole positions [Figure 8(b)].

When the hole is over regions with islands, we observe what we have previously reported: the decay is exponential for small times, whereas for larger times the power law emerges. On the other hand, when the hole is in the chaotic sea, *i.e.*, away from the main islands, the decay is slowed down, and we observe stretched exponentials. The difference is mainly because when the hole is placed partially or entirely over an island, it might destroy all orbits in the vicinity of this island.

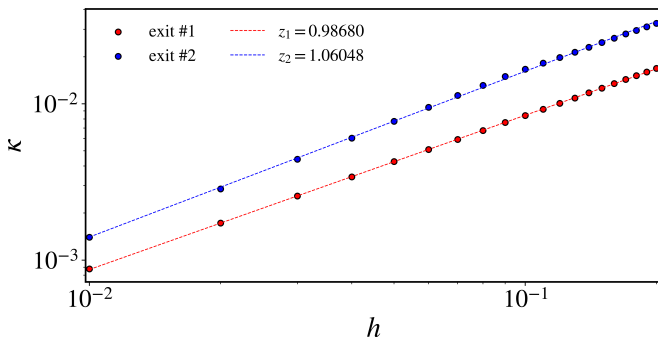


FIG. 6. (a) The escape rate for holes (red dots) #1 and (blue dots) #2 as a function of the hole size h . The dashed lines correspond to the optimal fit based on the function $f(h) \sim h^z$.

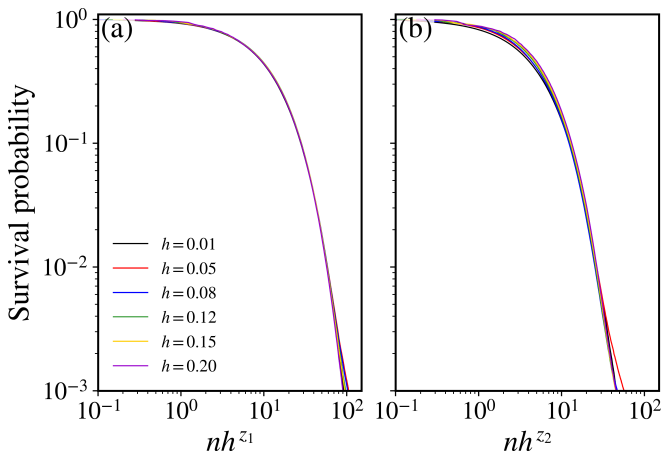


FIG. 7. The survival probability through holes (a) #1 and (b) #2 individually, for $\gamma = 3$, $\xi = 0.45$ and different values of h after the transformation $n \rightarrow nh^{z_i}$. Each z_i corresponds to the value shown in Figure 6. The curves overlap onto a single and universal plot.

In other words, it might destroy sticky regions and resonance zones that are responsible for slowing down the decay.

IV. ESCAPE BASINS

We have previously studied the escape of particles when one hole was open at a time. Next, we turn our attention to the escape dynamics when two holes are open simultaneously, and determine the escape basins for various hole sizes. We initialize an ensemble of $M = 10^6$ particles uniformly distributed in the phase space region delimited by $(\theta, \alpha) \in [0, \pi/3] \times [\pi/2 - 0.25, \pi + 0.25]$ for $\gamma = 3$ and $\xi = 0.45$. Each particle undergoes up to $N = 10^6$ collisions. We consider the same hole positions as in Section III (Figure 4). To construct the escape basin, we iterate each particle until it escapes from one of the two exits. If a particle escapes from hole #1 (#2), we color the corresponding point black (red). If a particle does not escape within the maximum number of iterations, we color the point white. Figure 9 shows the escape basins for six different hole size values h when two holes are open.

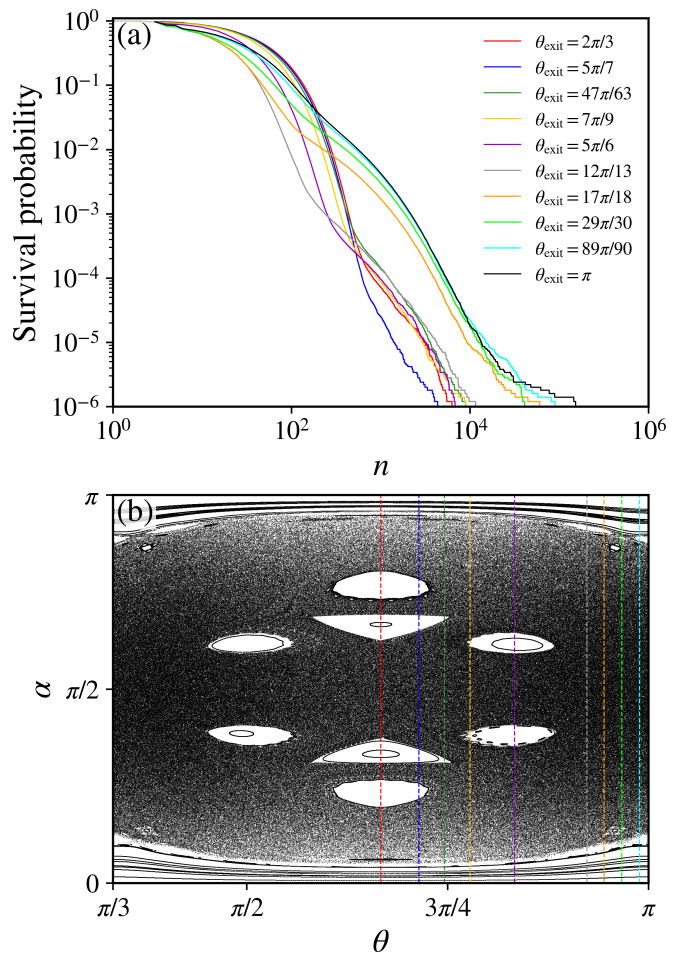


FIG. 8. (a) The survival probability for $\gamma = 3$, $\xi = 0.45$ and $h = 0.20$ for different hole positions marked by colored dashed lines in (b). We considered an ensemble of $M = 10^6$ initial conditions randomly distributed in $(\theta, \alpha) \in [0, \pi/3] \times [\pi/2 - 0.25, \pi/2 + 0.25]$.

For small hole sizes [Figure 9(a)], the black and red points are distributed almost at random, with nearly no discernible structure in the basin. As the hole sizes increase [Figure 9(b)-9(f)], the basins begin to exhibit a highly complex structure, characteristic of fractal basins. In order to quantify this complex structure, we apply the concept of basin entropy introduced by Daza and coworkers^{67,68}. This method has been successfully applied to a variety of problems in nonlinear dynamics, such as dissipative⁷⁴ and area-preserving⁷⁵⁻⁷⁷ non-twist systems, drift motion of charged plasma particles^{78,79}, chaotic scattering in Hamiltonian systems^{80,81} as well as relativistic scattering⁸². The basin entropy has been used to determine the fractal dimension of boundaries as well⁸³⁻⁸⁵.

The basin entropy quantifies the degree of uncertainty of a basin due to the fractality of the basin boundary. In order to calculate it, let us consider a bounded phase space region \mathcal{R} which contains N_A distinguishable asymptotic states. We discretize \mathcal{R} into a mesh of $N_T \times N_T$ boxes of linear size δ , and define an application $C : \mathcal{R} \rightarrow \mathbb{N}$ relating each initial condition to its asymptotic state. Daza *et al.*⁶⁷ called this application a color. Each box contains a large number N_p of initial condi-

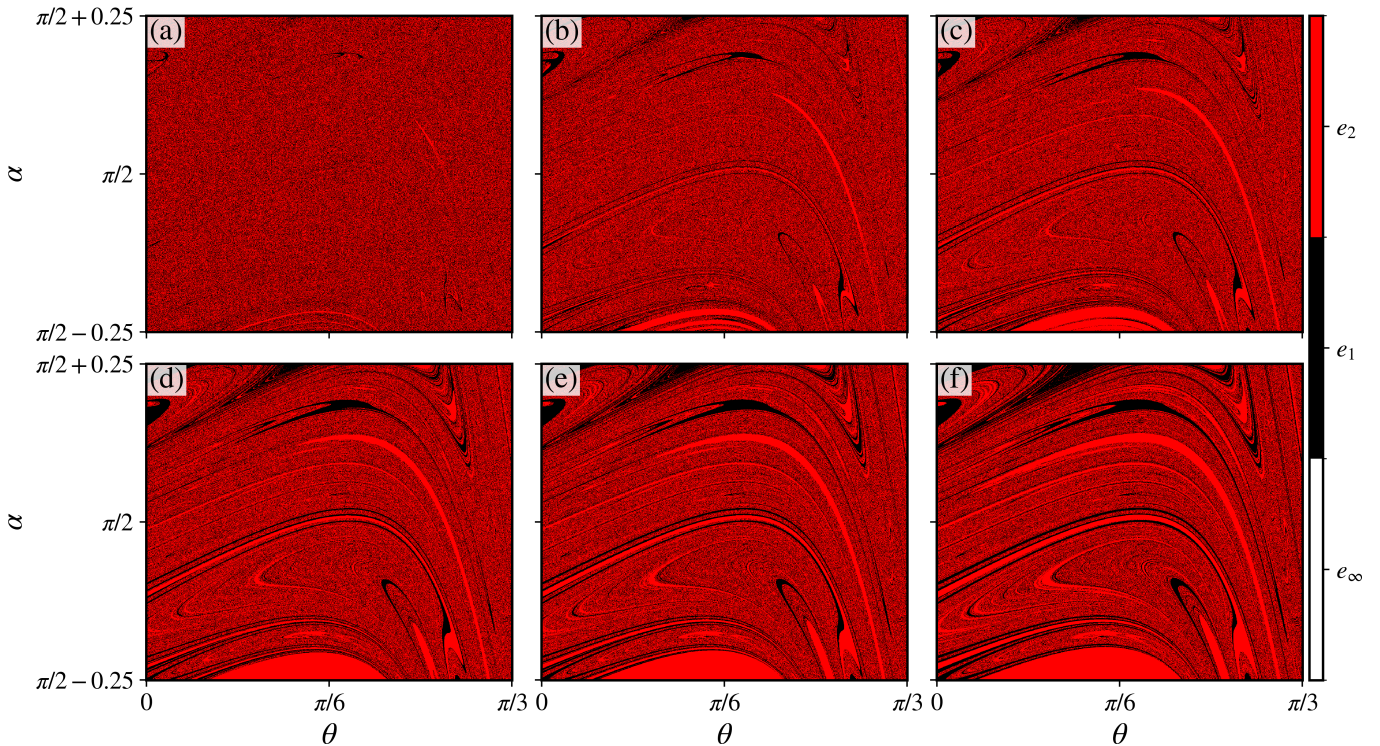


FIG. 9. The escape basin for the particles that escape through holes (black) #1 and (red) #2 for $\gamma = 3$, $\xi = 0.45$ and (a) $h = 0.01$, (b) $h = 0.05$, (c) $h = 0.08$, (d) $h = 0.12$, (e) $h = 0.15$, and (f) $h = 0.2$.

tions, each one leading to one of the N_A colors (asymptotic states). For each box i , we associate a probability p_{ij} of a color j to exist in this box and define the Shannon entropy of the i th box as

$$S_i = - \sum_{j=1}^{n_i} p_{ij} \log_2 p_{ij}, \quad (23)$$

where $n_i \in [1, N_A]$ is the number of different colors inside the i th box. The probability p_{ij} is simply the ratio between the number of points with color j and the total number of colors (initial conditions) in the box. In this paper, we consider a box with 25 initial conditions and cover the phase space region with 216×216 boxes, totalizing $1080^2 = 1166400$ initial conditions.

If the boxes covering \mathcal{R} are nonoverlapping, the entropy of the phase space region is simply the sum of the entropies of all boxes

$$S = \sum_{i=1}^{N_T^2} S_i, \quad (24)$$

and the basin entropy S_b and the basin boundary entropy S_{bb} are defined as

$$\begin{aligned} S_b &= \frac{S}{N_T^2}, \\ S_{bb} &= \frac{S}{N_b}, \end{aligned} \quad (25)$$

where N_b is the number of boxes that contain more than one color. The basin entropy, S_b , measures the basin degree of uncertainty, *i.e.*, for a single asymptotic state $S_b = 0$, whereas for N_A equiprobable asymptotic states, S_b has its maximum value of $S_b = \log_2 N_A$. On the other hand, the basin boundary entropy, S_{bb} , measures the uncertainty related only to the basin boundary. A fractality criterion has been provided by Daza *et al.*⁶⁷: if $S_{bb} > \log_2 2 = 1$, then the boundary is fractal. However, this is a sufficient but not necessary condition. In other words, if $S_{bb} > 1$, the boundary is fractal, however, if the boundary is fractal, S_{bb} might not satisfy this condition.

In our case, there are only three possible asymptotic states: the particles escape from either hole #1 or hole #2 or it does not escape at all (up to 10^6 collisions), hence $N_A = 3$. To calculate the entropies, we determine the escape basins for $\gamma = 3$ and $\xi \in [0.2, 0.9]$ for different hole sizes in the interval $h \in [0.01, 0.20]$ (Figure 10 and Video 1 from the Supplementary Material). The basin entropy for small h is large, as expected since the basins exhibit almost no ordered structure, as shown in Figure 9(a). As h increases, structures start to appear, and S_b and S_{bb} decreases, in general, but in a non-trivial fashion. This leads to an important question about such a measure: *Does the behavior of the basin entropy S_b remain invariant under variations in ξ and h ?* To address our inquiry, we first plot the basin entropy S_b as a function of the hole size h for different ξ values [Figure 11(a)]. We notice that S_b is described by an exponential function of the form $S_b(h; \xi) = Be^{-Ah}$. The analysis of the coefficients A and B as a function of ξ [Figures 11(b) and 11(c)] reveals a power

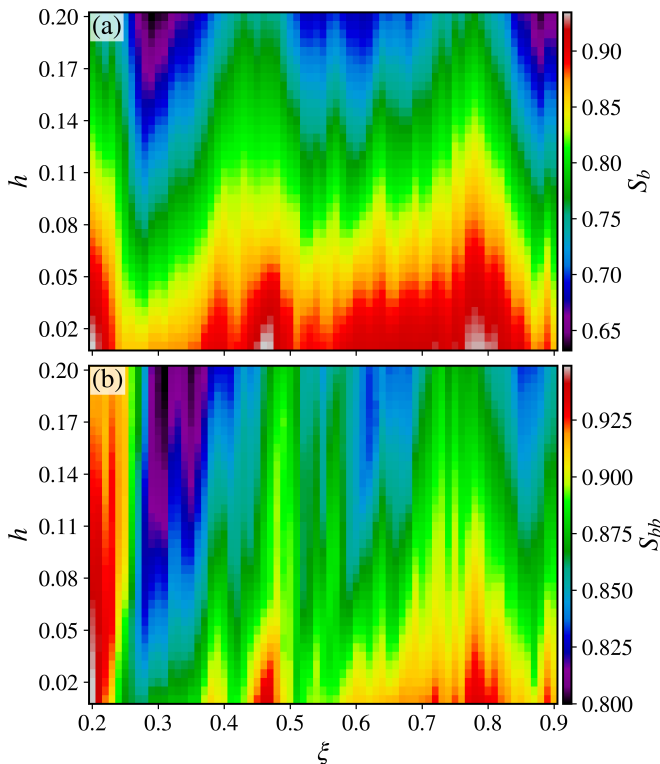


FIG. 10. The basin entropy, S_b , and the basin boundary entropy, S_{bb} , for the escape basin considering two holes (Figure 9) as a function of ξ and the hole sizes h with $\gamma = 3$.

law scaling for both of them, *i.e.*, $A(\xi) \sim \xi^{\zeta_1}$ and $B(\xi) \sim \xi^{\zeta_2}$, with $\zeta_1 = -0.91367$ and $\zeta_2 = 0.17284$. Armed with these exponents, we rescale the horizontal and vertical axis by the transformations $h \rightarrow h/\xi^{-\zeta_1}$ and $S_b \rightarrow S_b/\xi^{\zeta_2}$, respectively. These transformations align the curves in Figure 11(a) onto a single, and hence, universal plot [Figure 11(d)], indicating that S_b maintains its behavior regardless of ξ within the chosen interval.

V. FINAL REMARKS

We have examined the statistical properties of the escape of particles from a billiard system by introducing a hole on the billiard boundary. Firstly our analysis focused on the behavior of the survival probability, which gives us information regarding the fraction of particles that have not yet escaped from the billiard up to a certain number of collisions. We have demonstrated that when the hole overlaps with the larger stability islands, the survival probability obeys an exponential decay, whereas when the hole is placed in a region dominated by the chaotic sea, the decay follows a stretched exponential. Furthermore, in the cases where the hole is placed partially or entirely over a stability island, the survival probability exhibits scaling invariance with respect to the size of the exit, *i.e.*, the survival probability preserves its behavior regardless of the hole size.

Secondly, we have constructed escape basins for several

values of the control parameter ξ and the hole sizes h by introducing two holes simultaneously. We have demonstrated that for $h \ll 1$, the basins exhibit an almost random pattern, with very few definite structures. As h increases, the basins become increasingly complex with the emergence of multiple structures. In order to measure the complexity of these structures, we have applied the concept of basin entropy. We have found that both the basin entropy, S_b , and the basin boundary entropy, S_{bb} , are larger for smaller h for all values of ξ , as expected. Moreover, they decrease as h increases. The relation between these entropies and the parameters ξ and h is highly irregular and non-trivial. However, we have found that the basin entropy does maintain its behavior under parameter variations for a specific parameter interval. For $\xi \in [0.31, 0.38]$, the basin boundary exhibits an exponential decay with h , $S_b(h; \xi) = Be^{-Ah}$, and the coefficients A and B scale with ξ as a power law, with exponents $\zeta_1 = -0.91367$ and $\zeta_2 = 0.17284$. Upon rescaling the horizontal and vertical axis by $h \rightarrow h/\xi^{-\zeta_1}$ and $S_b \rightarrow S_b/\xi^{\zeta_2}$, respectively, we have demonstrated that the basin entropy curves align into a single, and universal, curve. This indicates that S_b is robust under variations of ξ . We would like to emphasize that while our basin entropy analysis mainly focused on boxes with 25 initial conditions, we also conducted simulations with 9, 16, 36, and 64 initial conditions. These simulations produced similar results, showing only minor variations in the exponents ζ_1 and ζ_2 . Due to this, we have chosen not to display them on this paper.

As a perspective of future works, we intend to study this billiard system with time-dependent holes as well as with a time-dependent boundary.

DECLARATION OF COMPETING INTEREST

The authors declare that they have no known competing financial interests or personal relationships that could have appeared to influence the work reported in this paper.

CODE AVAILABILITY

The source code to reproduce the results reported in this paper is freely available on the Zenodo archive⁸⁶ and in the GitHub repository⁸⁷.

ACKNOWLEDGMENTS

This work was supported by the Araucária Foundation, the Coordination of Superior Level Staff Improvement (CAPES), the National Council for Scientific and Technological Development (CNPq), under Grant Nos. 01318/2019-0, 309670/2023-3, and by the São Paulo Research Foundation, under Grant Nos. 2019/14038-6, 2022/03612-6, 2023/08698-9.

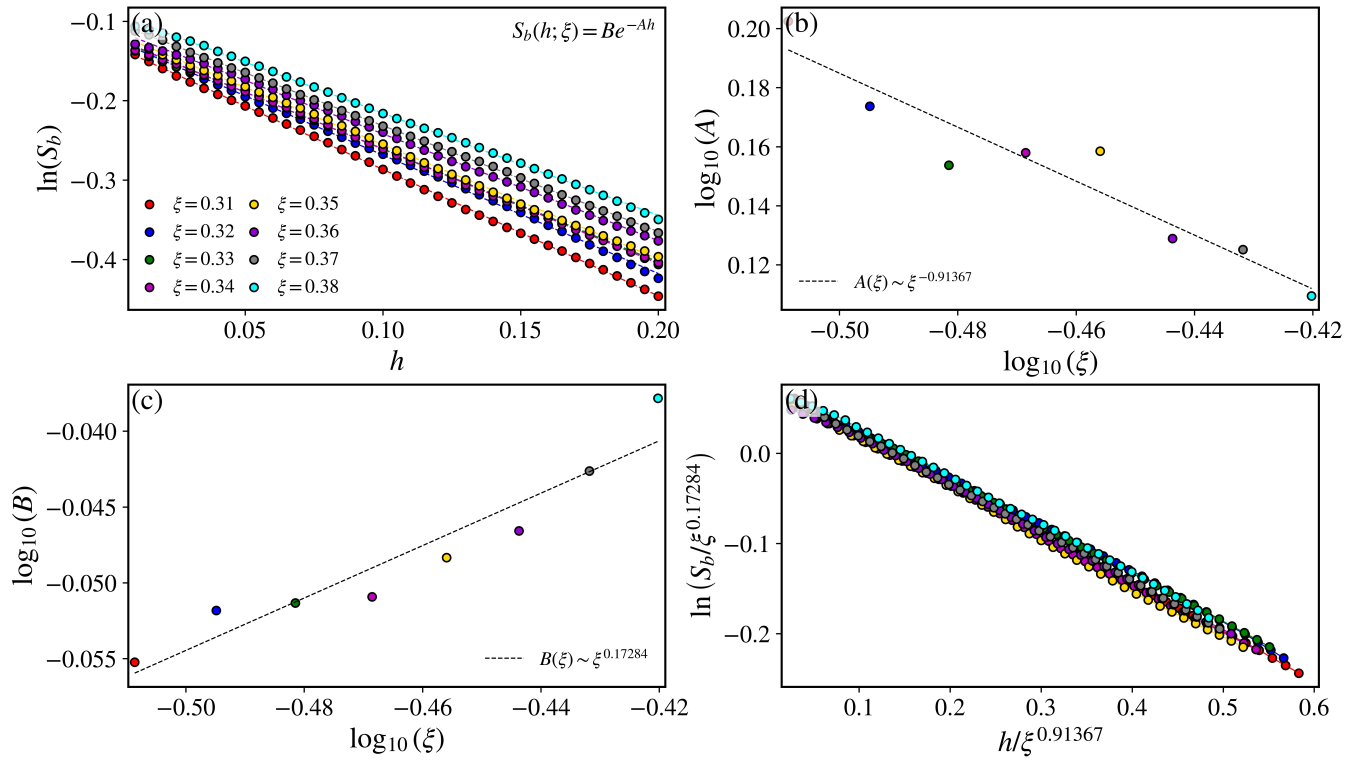


FIG. 11. (a) The basin entropy, S_b , as a function of the holes size, h , for different values of ξ (colored dots). The dashed lines correspond to the optimal fit based on the function $S_b(h; \xi) = Be^{-Ah}$. (b) and (c) The coefficients A and B obtained from the fitting in (a) as a function of ξ . Both coefficients scale with ξ as a power law and the dashed lines correspond to the optimal fit based on the function $f(\xi) \sim \xi^\zeta$. (d) The overlap of S_b onto a single and universal plot after the transformations $h \rightarrow h/\xi^{0.91367}$ and $S_b \rightarrow S_b/\xi^{0.17284}$.

- ¹A. J. Lichtenberg and M. A. Lieberman, *Regular and chaotic dynamics*, Applied Mathematical Sciences, Vol. 38 (Springer-Verlag, 1992).
- ²R. S. Mackay, J. D. Meiss, and I. C. Percival, "Transport in Hamiltonian systems," *Physica D: Nonlinear Phenomena* **13**, 55–81 (1984).
- ³J. D. Meiss and E. Ott, "Markov-tree model of intrinsic transport in Hamiltonian systems," *Phys. Rev. Lett.* **55**, 2741–2744 (1985).
- ⁴J. D. Meiss and E. Ott, "Markov tree model of transport in area-preserving maps," *Physica D: Nonlinear Phenomena* **20**, 387–402 (1986).
- ⁵G. Contopoulos, "Orbits in Highly Perturbed Dynamical Systems. 111. Nonperiodic Orbits," *The Astronomical Journal* **76**, 147 (1971).
- ⁶C. F. Karney, "Long-time correlations in the stochastic regime," *Physica D: Nonlinear Phenomena* **8**, 360–380 (1983).
- ⁷J. D. Meiss, J. R. Cary, C. Grebogi, J. D. Crawford, A. N. Kaufman, and H. D. Abarbanel, "Correlations of periodic, area-preserving maps," *Physica D: Nonlinear Phenomena* **6**, 375–384 (1983).
- ⁸B. Chirikov and D. Shepelyansky, "Correlation properties of dynamical chaos in Hamiltonian systems," *Physica D: Nonlinear Phenomena* **13**, 395–400 (1984).
- ⁹C. Efthymiopoulos, G. Contopoulos, N. Voglis, and R. Dvorak, "Stickiness and cantori," *Journal of Physics A: Mathematical and General* **30**, 8167 (1997).
- ¹⁰G. Contopoulos and M. Harsoula, "Stickiness in chaos," *International Journal of Bifurcation and Chaos* **18**, 2929–2949 (2008).
- ¹¹G. Cristadoro and R. Ketzmerick, "Universality of algebraic decays in Hamiltonian systems," *Phys. Rev. Lett.* **100**, 184101 (2008).
- ¹²G. Contopoulos and M. Harsoula, "Stickiness effects in conservative systems," *International Journal of Bifurcation and Chaos* **20**, 2005–2043 (2010).
- ¹³R. S. MacKay, J. D. Meiss, and I. C. Percival, "Stochasticity and transport in Hamiltonian systems," *Phys. Rev. Lett.* **52**, 697–700 (1984).
- ¹⁴F. Vivaldi, G. Casati, and I. Guarneri, "Origin of long-time tails in strongly chaotic systems," *Phys. Rev. Lett.* **51**, 727–730 (1983).
- ¹⁵Č. Lozej and M. Robnik, "Structure, size, and statistical properties of chaotic components in a mixed-type Hamiltonian system," *Phys. Rev. E* **98**, 022220 (2018).
- ¹⁶G. M. Zaslavskii and B. V. Chirikov, "Stochastic instability of non-linear oscillations," *Soviet Physics Uspekhi* **14**, 549 (1972).
- ¹⁷G. M. Zaslavsky, M. Edelman, and B. A. Niyazov, "Self-similarity, renormalization, and phase space nonuniformity of Hamiltonian chaotic dynamics," *Chaos: An Interdisciplinary Journal of Nonlinear Science* **7**, 159–181 (1997).
- ¹⁸G. Zaslavsky, "Chaos, fractional kinetics, and anomalous transport," *Physics Reports* **371**, 461–580 (2002).
- ¹⁹G. M. Zaslavsky, *Hamiltonian chaos and fractional dynamics* (Oxford University Press, USA, 2005).
- ²⁰V. Afraimovich and G. M. Zaslavsky, "Fractal and multifractal properties of exit times and Poincaré recurrences," *Phys. Rev. E* **55**, 5418–5426 (1997).
- ²¹E. G. Altmann, A. E. Motter, and H. Kantz, "Stickiness in mushroom billiards," *Chaos: An Interdisciplinary Journal of Nonlinear Science* **15**, 033105 (2005).
- ²²H. Tanaka and A. Shudo, "Recurrence time distribution in mushroom billiards with parabolic hat," *Phys. Rev. E* **74**, 036211 (2006).
- ²³E. G. Altmann, A. E. Motter, and H. Kantz, "Stickiness in Hamiltonian systems: From sharply divided to hierarchical phase space," *Phys. Rev. E* **73**, 026207 (2006).
- ²⁴R. Venegeroles, "Universality of algebraic laws in Hamiltonian systems," *Phys. Rev. Lett.* **102**, 064101 (2009).
- ²⁵C. V. Abud and R. E. de Carvalho, "Multifractality, stickiness, and recurrence-time statistics," *Phys. Rev. E* **88**, 042922 (2013).
- ²⁶Č. Lozej, "Stickiness in generic low-dimensional Hamiltonian systems: A recurrence-time statistics approach," *Phys. Rev. E* **101**, 052204 (2020).

- ²⁷Y.-C. Lai, M. Ding, C. Grebogi, and R. Blümel, “Algebraic decay and fluctuations of the decay exponent in Hamiltonian systems,” *Phys. Rev. A* **46**, 4661–4669 (1992).
- ²⁸E. G. Altmann and T. Tél, “Poincaré recurrences and transient chaos in systems with leaks,” *Phys. Rev. E* **79**, 016204 (2009).
- ²⁹V. A. Avetisov and S. K. Nechaev, “Chaotic Hamiltonian systems: Survival probability,” *Phys. Rev. E* **81**, 046211 (2010).
- ³⁰C. P. Dettmann and E. D. Leonel, “Escape and transport for an open bouncer: Stretched exponential decays,” *Physica D: Nonlinear Phenomena* **241**, 403–408 (2012).
- ³¹E. D. Leonel and C. P. Dettmann, “Recurrence of particles in static and time varying oval billiards,” *Physics Letters A* **376**, 1669–1674 (2012).
- ³²A. L. P. Livorati, T. Kroetz, C. P. Dettmann, I. L. Caldas, and E. D. Leonel, “Stickiness in a bouncer model: A slowing mechanism for Fermi acceleration,” *Phys. Rev. E* **86**, 036203 (2012).
- ³³A. L. P. Livorati, O. Georgiou, C. P. Dettmann, and E. D. Leonel, “Escape through a time-dependent hole in the doubling map,” *Phys. Rev. E* **89**, 052913 (2014).
- ³⁴J. A. Méndez-Bermúdez, A. J. Martínez-Mendoza, A. L. P. Livorati, and E. D. Leonel, “Leaking of trajectories from the phase space of discontinuous dynamics,” *Journal of Physics A: Mathematical and Theoretical* **48**, 405101 (2015).
- ³⁵N. B. de Faria, D. S. Tavares, W. C. S. de Paula, E. D. Leonel, and D. G. Ladeira, “Transport of chaotic trajectories from regions distant from or near to structures of regular motion of the Fermi-Ulam model,” *Phys. Rev. E* **94**, 042208 (2016).
- ³⁶A. L. Livorati, M. S. Palmero, G. Díaz-I, C. P. Dettmann, I. L. Caldas, and E. D. Leonel, “Investigation of stickiness influence in the anomalous transport and diffusion for a non-dissipative Fermi-Ulam model,” *Communications in Nonlinear Science and Numerical Simulation* **55**, 225–236 (2018).
- ³⁷D. Borin, A. L. P. Livorati, and E. D. Leonel, “An investigation of the survival probability for chaotic diffusion in a family of discrete Hamiltonian mappings,” *Chaos, Solitons & Fractals* **175**, 113965 (2023).
- ³⁸E. D. Leonel, *Scaling Laws in Dynamical Systems*, 1st ed. (Springer Singapore, 2021).
- ³⁹E. D. Leonel, P. V. E. McClintock, and J. K. L. da Silva, “Fermi-Ulam accelerator model under scaling analysis,” *Phys. Rev. Lett.* **93**, 014101 (2004).
- ⁴⁰E. D. Leonel, “Corrugated waveguide under scaling investigation,” *Phys. Rev. Lett.* **98**, 114102 (2007).
- ⁴¹A. L. P. Livorati, D. G. Ladeira, and E. D. Leonel, “Scaling investigation of Fermi acceleration on a dissipative bouncer model,” *Phys. Rev. E* **78**, 056205 (2008).
- ⁴²J. A. de Oliveira, R. A. Bizão, and E. D. Leonel, “Finding critical exponents for two-dimensional Hamiltonian maps,” *Phys. Rev. E* **81**, 046212 (2010).
- ⁴³E. D. Leonel and P. V. E. McClintock, “Scaling properties for a classical particle in a time-dependent potential well,” *Chaos: An Interdisciplinary Journal of Nonlinear Science* **15**, 033701 (2005).
- ⁴⁴J. A. de Oliveira, L. T. Montero, D. R. da Costa, J. A. Méndez-Bermúdez, R. O. Medrano-T, and E. D. Leonel, “An investigation of the parameter space for a family of dissipative mappings,” *Chaos: An Interdisciplinary Journal of Nonlinear Science* **29**, 053114 (2019).
- ⁴⁵E. D. Leonel, J. Penalva, R. M. Teixeira, R. N. Costa Filho, M. R. Silva, and J. A. de Oliveira, “A dynamical phase transition for a family of Hamiltonian mappings: A phenomenological investigation to obtain the critical exponents,” *Physics Letters A* **379**, 1808–1815 (2015).
- ⁴⁶J. A. de Oliveira, C. P. Dettmann, D. R. da Costa, and E. D. Leonel, “Scaling invariance of the diffusion coefficient in a family of two-dimensional Hamiltonian mappings,” *Phys. Rev. E* **87**, 062904 (2013).
- ⁴⁷D. F. Oliveira, M. Robnik, and E. D. Leonel, “Statistical properties of a dissipative kicked system: Critical exponents and scaling invariance,” *Physics Letters A* **376**, 723–728 (2012).
- ⁴⁸J. A. Méndez-Bermúdez, R. Aguilar-Sánchez, J. M. Sigarreta, and E. D. Leonel, “Scaling properties of the action in the riemann-liouville fractional standard map,” *Phys. Rev. E* **109**, 034214 (2024).
- ⁴⁹D. Borin, “Caputo fractional standard map: Scaling invariance analyses,” *Chaos, Solitons & Fractals* **181**, 114597 (2024).
- ⁵⁰S. Tabachnikov, *Geometry and billiards*, Vol. 30 (American Mathematical Soc., 2005).
- ⁵¹L. A. Bunimovich, “Mechanisms of chaos in billiards: dispersing, defocusing and nothing else,” *Nonlinearity* **31**, R78 (2018).
- ⁵²Y. G. Sinai, “Dynamical systems with elastic reflections,” *Russian Mathematical Surveys* **25**, 137 (1970).
- ⁵³L. A. Bunimovich, “On ergodic properties of certain billiards,” *Functional Analysis and Its Applications* **8**, 254–255 (1974).
- ⁵⁴M. Robnik, “Classical dynamics of a family of billiards with analytic boundaries,” *Journal of Physics A: Mathematical and General* **16**, 3971 (1983).
- ⁵⁵L. A. Bunimovich, “Mushrooms and other billiards with divided phase space,” *Chaos: An Interdisciplinary Journal of Nonlinear Science* **11**, 802–808 (2001).
- ⁵⁶D. R. da Costa, M. S. Palmero, J. Méndez-Bermúdez, K. C. Iarosz, J. D. Szezech Jr, and A. M. Batista, “Tilted-hat mushroom billiards: Web-like hierarchical mixed phase space,” *Communications in Nonlinear Science and Numerical Simulation* **91**, 105440 (2020).
- ⁵⁷M. Berry, “Quantum chaology, not quantum chaos,” *Physica Scripta* **40**, 335 (1989).
- ⁵⁸G. Casati and T. Prosen, “The quantum mechanics of chaotic billiards,” *Physica D: Nonlinear Phenomena* **131**, 293–310 (1999).
- ⁵⁹A. H. Barnett and T. Betcke, “Quantum mushroom billiards,” *Chaos: An Interdisciplinary Journal of Nonlinear Science* **17**, 043125 (2007).
- ⁶⁰D. D. de Menezes, M. Jar e Silva, and F. M. de Aguiar, “Numerical experiments on quantum chaotic billiards,” *Chaos: An Interdisciplinary Journal of Nonlinear Science* **17**, 023116 (2007).
- ⁶¹F. Zanetti, E. Vicentini, and M. da Luz, “Eigenstates and scattering solutions for billiard problems: A boundary wall approach,” *Annals of Physics* **323**, 1644–1676 (2008).
- ⁶²M. V. Deryabin and L. D. Pustyl’nikov, “On generalized relativistic billiards in external force fields,” *Letters in Mathematical Physics* **63**, 195–207 (2003).
- ⁶³M. V. Deryabin and L. D. Pustyl’nikov, “Exponential attractors in generalized relativistic billiards,” *Communications in Mathematical Physics* **248**, 527–552 (2004).
- ⁶⁴R. S. Pinto and P. S. Letelier, “Fermi acceleration in driven relativistic billiards,” *Physics Letters A* **375**, 3273–3278 (2011).
- ⁶⁵K.-i. Arita and M. Brack, “Anomalous shell effect in the transition from a circular to a triangular billiard,” *Phys. Rev. E* **77**, 056211 (2008).
- ⁶⁶D. R. da Costa, A. Fujita, M. R. Sales, J. D. Szezech, and A. M. Batista, “Dynamical properties for a tunable circular to polygonal billiard,” *Brazilian Journal of Physics* **52**, 75 (2022).
- ⁶⁷A. Daza, A. Wagemakers, B. Georgeot, D. Guéry-Odelin, and M. A. F. Sanjuán, “Basin entropy: a new tool to analyze uncertainty in dynamical systems,” *Scientific Reports* **6**, 31416 (2016).
- ⁶⁸A. Daza, B. Georgeot, D. Guéry-Odelin, A. Wagemakers, and M. A. F. Sanjuán, “Chaotic dynamics and fractal structures in experiments with cold atoms,” *Phys. Rev. A* **95**, 013629 (2017).
- ⁶⁹D. R. da Costa, M. Hansen, M. R. Silva, and E. D. Leonel, “Tangent method and some dynamical properties of an oval-like billiard,” *International Journal of Bifurcation and Chaos* **32**, 2250052 (2022).
- ⁷⁰For the chosen parameter values, there are only a few very small stability islands within this region (not shown). If a particle happens to fall within one of these small islands, we exclude it from the analysis. This exclusion does not significantly impact the overall behavior of the survival probability, as the number of discarded particles is much smaller than the total number of particles in the ensemble.
- ⁷¹C. P. Dettmann, “Recent advances in open billiards with some open problems,” in *Frontiers in the Study of Chaotic Dynamical Systems with Open Problems* (World Scientific, 2011) Chap. 11, pp. 195–218.
- ⁷²M. Hansen, R. Egydio de Carvalho, and E. D. Leonel, “Influence of stability islands in the recurrence of particles in a static oval billiard with holes,” *Physics Letters A* **380**, 3634–3639 (2016).
- ⁷³M. Hansen, D. R. da Costa, I. L. Caldas, and E. D. Leonel, “Statistical properties for an open oval billiard: An investigation of the escaping basins,” *Chaos, Solitons & Fractals* **106**, 355–362 (2018).
- ⁷⁴M. Mugnaine, A. M. Batista, I. L. Caldas, J. Szezech, José D., R. E. de Carvalho, and R. L. Viana, “Curry–Yorke route to shearless attractors and coexistence of attractors in dissipative nontwist systems,” *Chaos: An Interdisciplinary Journal of Nonlinear Science* **31**, 023125 (2021).

- ⁷⁵M. Mugnaine, A. C. Mathias, M. S. Santos, A. M. Batista, J. D. Szezech, and R. L. Viana, “Dynamical characterization of transport barriers in non-twist Hamiltonian systems,” *Phys. Rev. E* **97**, 012214 (2018).
- ⁷⁶A. C. Mathias, M. Mugnaine, M. S. Santos, J. D. Szezech, I. L. Caldas, and R. L. Viana, “Fractal structures in the parameter space of nontwist area-preserving maps,” *Phys. Rev. E* **100**, 052207 (2019).
- ⁷⁷L. C. Souza, A. C. Mathias, P. Haerter, and R. L. Viana, “Basin entropy and shearless barrier breakup in open non-twist Hamiltonian systems,” *Entropy* **25**, 1142 (2023).
- ⁷⁸A. Mathias, R. Viana, T. Kroetz, and I. Caldas, “Fractal structures in the chaotic motion of charged particles in a magnetized plasma under the influence of drift waves,” *Physica A: Statistical Mechanics and its Applications* **469**, 681–694 (2017).
- ⁷⁹L. C. Souza, A. C. Mathias, I. L. Caldas, Y. Elskens, and R. L. Viana, “Fractal and Wada escape basins in the chaotic particle drift motion in tokamaks with electrostatic fluctuations,” *Chaos: An Interdisciplinary Journal of Nonlinear Science* **33**, 083132 (2023).
- ⁸⁰E. E. Zotos, “An overview of the escape dynamics in the Hénon–Heiles Hamiltonian system,” *Meccanica* **52**, 2615–2630 (2017).
- ⁸¹A. R. Nieto, E. E. Zotos, J. M. Seoane, and M. A. F. Sanjuán, “Measuring the transition between nonhyperbolic and hyperbolic regimes in open Hamiltonian systems,” *Nonlinear Dynamics* **99**, 3029–3039 (2020).
- ⁸²J. D. Bernal, J. M. Seoane, and M. A. F. Sanjuán, “Uncertainty dimension and basin entropy in relativistic chaotic scattering,” *Phys. Rev. E* **97**, 042214 (2018).
- ⁸³A. Puy, A. Daza, A. Wagemakers, and M. A. Sanjuán, “A test for fractal boundaries based on the basin entropy,” *Communications in Nonlinear Science and Numerical Simulation* **95**, 105588 (2021).
- ⁸⁴A. Gusso and L. E. de Mello, “Fractal dimension of basin boundaries calculated using the basin entropy,” *Chaos, Solitons & Fractals* **153**, 111532 (2021).
- ⁸⁵A. Daza, A. Wagemakers, and M. A. F. Sanjuán, “Unpredictability and basin entropy,” *Europhysics Letters* **141**, 43001 (2023).
- ⁸⁶M. Rolim Sales, “mrolims/tunable-billiard: v1.0.1,” (2024).
- ⁸⁷M. Rolim Sales, “mrolims/tunable-billiard,” (2024).